Journal of Manufacturing Processes 67 (2021) 503–512

Contents lists available at ScienceDirect

Journal of Manufacturing Processes

journal homepage: www.elsevier.com/locate/manpro

# The impact of thermo-mechanical processing routes on product quality in integrated aluminium tube bending process

J. Ma *, T. Welo *, D. Wan

*Department of Mechanical and Industrial Engineering, Norwegian University of Science and Technology, Trondheim, 7491, Norway*

ARTICLE INFO

*Keywords:*
Tube bending
Integrated processing route
Aluminium alloy

ABSTRACT

In response to the increased demand for high dimensional accuracy and mechanical properties of formed metal products, this research aims to provide new insights into the impact of thermo-mechanical processing routes on quality in integrated bending process for heat-treatable aluminium tubes. Based on carefully controlled experiments with four representative processing routes, including R1: solution-heat-treatment (SHT) → bending → artificial aging (AA), R2: SHT → bending → natural aging (NA), R3: SHT → NA → bending → AA, and R4: SHT → NA → bending, the impact of these routes on final geometrical dimensions and mechanical properties of bent parts is thoroughly evaluated. As compared with R2 and R4 routes employing naturally-aged tubes in the bending operation, R1 and R3 routes with bending of SHT tubes significantly reduce both springback by 50 % and wall-thinning by 26 %. Considering product strength, however, for the routes with AA, R3 can achieve 16 % improvement of the hardness as compared to R1; for the routes without AA resulting in products in T4-temper, R4 can make the average hardness 20 % higher than R2. Moreover, R1 and R3 routes can make a more uniform hardness distribution in the cross-section of bent tubes than the two others, meaning that AA reduces the hardening effect of pre-deformation. All these findings provide a knowledge basis for the selection of suitable processing routes as well as the design of new, customized processing routes for the efficient manufacture of value-added aluminium tubular products.

## 1. Introduction

Aluminium alloys are playing a core role in metal forming for the sustainable and lightweight design of products to meet the stringent demands for reduced fuel consumption and $CO_2$ emissions [1]. Bent aluminium alloy tubes, profiles, and extrusions, as one type of important lightweight structures in aluminium family, are widely used in many industrial fields such as automobile, highway train and aerospace, typically serving as low-weight mass/heat-transferring systems or load-bearing structures [2]. Especially in the automobile industry, heat-treatable Al-Mg-Si aluminium alloys have gained great popularity due to their favorable strength-to-density ratio in combination with high corrosion resistance, weldability and recyclability [3].

In today's competitive market, product requirements have become increasingly more stringent and important. For the design and development of products made by metal forming, both 'dimensional accuracy-driven' and 'product property-driven' requirements must be satisfied to assure functional performance of products [4]. Important concerns associated with the former in tube bending processes, include wall-thinning (or cracks or other failures), ovalization of cross-section, springback, etc., causing a series of problems to subsequent processing operations as well as to functional performance of final products [5]. Taking the springback for example, it increases tolerance bands of final products, variability in assembly and durability of products [6]. From the concern of product performance taking mechanical properties as an example, favorable strength, residual stresses, and multiple other influential factors must be defined to ensure high in-situ performance [7]. For example, pressure-resistance (load-bearing) capability is one of key performance features of tubular parts, which not only depends on the strength of formed parts but is significantly affected by the geometrical dimensions of bent tubes such as wall-thinning [8].

Up to now, different tube bending methods have been developed, for example, rotary draw bending (RDB) [9], push bending [10], roll bending [11], stretch bending [12], and free-form bending [13,14]. To further improve bendability for hard-to-deform materials, heat-assisted bending processes have also been developed based on the above bending methods [15–18]. Moreover, Zhou et al. [19] proposed a differential velocity sideways extrusion process, which enables the manufacturing of

* Corresponding authors.
*E-mail addresses:* jun.ma@ntnu.no (J. Ma), torgeir.welo@ntnu.no (T. Welo).

https://doi.org/10.1016/j.jmapro.2021.05.015
Received 30 January 2021; Received in revised form 31 March 2021; Accepted 4 May 2021

curved aluminium profiles with fine grains and high strength. Lin et al. [20] recently proposed a radial hydro-forging bending process, which could alleviate the complication of springback for bent tubular components. These methods greatly contribute to the manufacture of aluminium bent tubular parts for different application purposes. Notwithstanding, many issues related to dimensional accuracy and mechanical properties are still challenging to control. Seeking advanced processing approaches to address the above issues is still important and imperative. To achieve this goal, an alternative, effective strategy is integrating forming operations and thermal treatments, seeking more optimal conditions for a given application and production setup. Such a strategy is particularly important to the products made of heat-treatable aluminium alloys, as the unique strength response under different thermal treatments provides additional flexibility to proactively control dimensional accuracy influenced by e.g. springback and the mechanical properties of the product strength, as well as improve the formability. At the same time, this strategy has a potential to positively affect production efficiency, process capability, and manufacturing cost, as compared to some other methods.

To design feasible and efficient integrated processes for high-value aluminium bent tubes, the complex effect of thermal processing route (or history) on geometrical and mechanical characteristics must be known. At present, extensive efforts have been made to develop the integrated processing routes by combing conventional forming operations together with thermal treatments such as solution-heat-treatment (SHT) and artificial aging (AA). A typical example is the Hot Form and Quench (HFQ®) process proposed by Lin et al. [21], which has been developed as a leading-edge technique in hot stamping of high-strength aluminium panels. In this process, the sheet blank is solution-heat-treated to dissolve precipitates and inclusions to obtain a more ductile behavior, before being quickly transferred to the stamping operation and instantly quenched in cold dies. The AA operation is normally the final thermal processing step for heat-treatable alloys used to increase the strength of formed parts supplied in T6 (or T5) condition [22]. As springback is closely related to the yield strength-to-Young's modulus ratio, the SHT step enables a significant decrease of springback due to the lower material strength. At the same time, the SHT improves the ductility of aluminium alloys, which enables the forming performance of hard-to-form products. In order to improve the control of dimensional accuracy and mechanical product properties, while providing efficient and economic production for the processes, optimization of upstream and in-line parameters is needed, in particular, the thermal processing ones [23]. For example, Li et al. [24] proposed a fast aging strategy for stamped heat-treatable alloys, in which a two-stage aging scheme including pre-aging at a higher temperature and subsequent paint bake stage at relatively low temperatures, thus reduce the aging time needed as compared with the conventional AA method at a constant temperature. However, these studies are focused on the stamping of sheet parts, and there is a lack of such type of studies on the process design of aluminium tube bending. Even though, the above studies provide a useful reference to explore and design more efficient processes with integrating thermal processing routes in conventional aluminium tube bending. As the deformation characteristics in tube bending are different from those in sheet stamping, the contribution of these thermal processing routes to the improvement of overall quality characteristics may also different and are not clearly understood yet.

Several attempts have also been made to design or customize thermal processing routes for tube bending processes. To name a few, Bourget et al. [25] examined the influence of heat treatment parameters on mechanical properties and bendability of AA6063 cold-drawn aluminium tubes, showing that the latter is significantly influenced by heat treatment applied to the tubes prior to forming. Also, elongation at fracture measured in a uniaxial tensile test was found to have strong correlation with tube bendability in that work. However, in that work, only the effect of a single heat treatment step before forming on bendability was considered, and more detailed geometrical dimensions and mechanical properties of bent shapes were not concerned either. Sert et al. [26] investigated the effect of heat treatment of T6, T4, and O tempers on the bending behavior of 6082 tubes in three-point bending. However, the main emphasis of this work was put on the effect of heat treatment on specific energy absorption capability, and the forming quality of bent tubes were not concerned. Ma et al. [27] studied the effect of pre-bend natural aging (NA) time on springback of AA6060 alloy tubes in rotary draw bending (RDB), showing that springback is very sensitive to the NA time at room temperature. However, in that work, only the springback related to the pre-bend shelf life is concerned. How the processing route influenced other critical geometrical dimensions, like wall-thinning and cross-sectional ovalization, as well as mechanical properties, were not investigated in that work. In particular, there is a lack of understanding on the effect of heat treatments after forming as well as the coupled effect thermal processing routes throughout the entire process on the quality of bent tubular parts.

The body of research on the influence of thermal processing routes on quality of formed aluminium components is obviously more extensive than the above-summarized ones, and many works not mentioned above have made important contributions to the understanding of the topic. However, very few relevant studies of how the thermo-mechanical processing route affects both geometrical dimensions and mechanical properties in the bending of aluminium tubes, are found. Thus, lack of knowledge in this research field has put a restriction to effective design and development of aluminium tube bending processes, considering the thermo-mechanical history effect.

Aiming to make a contribution to filling this research gap, the present study is done to provide new insights into the impact of thermal processing routes in the integrated bending process of aluminium alloy tubes. Using AA6060 alloy tubes as the case material, a series of processing routes are carefully designed and controlled to study how thermal treatments, including SHT, AA, and NA, in combination with rotary draw bending, affect product quality. Particular focus is made on geometrical dimensions of the bent tube—including springback, wall thickness variation, and ovalization of cross-section—as well as hardness distributions along the perimeter of the cross-section and the relationships to different thermal processing routes. The findings in this research improve the understanding of the impact of thermal processing on geometrical dimensions and properties in aluminium tube bending, which forms the basis for enabling the design of feasible and efficient processes for manufacturing of high-quality aluminium alloy products.

The remainder of the paper is organized as follows. Section 2 presents the experimental procedure including the design of processing routes, measurement methods, and a 'NaMo' simulation of material properties. Section 3 analyzes the influence of different processing routes on dimensional accuracy like springback, wall-thinning, and ovalization of cross-section, and strength of bent shapes. Finally, Section 4 summarizes the conclusions and provides an outlook for future research.

## 2. Methodology

In this study, commonly used AA6060 tubes with nominal outer diameter ($D$) of 16 mm and wall thickness ($t$) of 1.7 mm are used to explore the impact of thermal processing routes on the product quality of bent parts. Since the diameter-to-thickness ratio ($D/t = 9.41$) is less than 20, the tubular section used in this work is normally categorized as thick-walled. The as-received tubes are supplied by the Hydro ASA company and manufactured by standard hot-extrusion process and naturally aged to stabilized T4-temper condition prior to arrival. The nominal chemical composition of AA6060 is listed in Table 1. It should be noted that the given geometry of tube used in this study is taken as a case material to explore the impacts related to processing routes. The principle of this integrated forming strategy presented in Section 2.1 is the thermal treatment-based manipulation of mechanical properties of materials and formed parts. Thus, this strategy is not limited to a certain

**Table 1**
Nominal chemical composition of AA6060 (in wt.%) [28].

| Si | Fe | Cu | Mn | Mg | Cr | Zn | Ti | Other |
|---|---|---|---|---|---|---|---|---|
| 0.3~0.6 | 0.1~0.3 | 0.1 | 0.1 | 0.35~0.6 | 0.05 | 0.15 | 0.1 | 0.15 |

tube geometry but is applicable to manufacturing bent parts in AA6060 with a wide range of geometries.

### 2.1. Integrated processing routes

The integrated processing strategy for aluminium bent tubes is shown in Fig. 1. It integrates cold bending operation and thermal treatments, seeking more optimal combinations for improved geometrical dimensions, mechanical properties, as well as formability. In this study, four processing routes are carefully designed to explore the effect of thermo-mechanical loading history on geometrical dimensions and product strength in AA6060 alloy tube bending. To make the entire experimental process more controllable, SHT and water quenching are performed for the entire batch of the T4-temper material received. Hence, the SHT with the subsequent water quenching is used as the initial step for all four processing routes to ensure the same basis, resembling the extrusion and cooling process used in industry for this alloy. Following this step, different combinations of thermal/natural aging treatments and cold bending are conducted.

Referring to Fig. 2, the four processing routes are briefly introduced as follows:

- Route I consists of SHT, immediate cold bending, and post-bend AA in sequence, which in short is described as 'R1'.
- Route II consists of SHT, immediate cold bending, and post-bend NA for 180 days to T4-temper, which in short is described as 'R2'. No post-bend AA was performed.
- Route III consists of SHT followed by 180 days storage to T4-temper, cold bending, and AA in sequence, which is in short described as 'R3'.
- Route IV consists of SHT, storage at room temperature for 180 days to T4-temper, and cold bending in sequence, which is in short described as 'R4'. No post-bend AA was performed.

It should be noted that, in R1 and R2 processes, the transfer time from SHT to bending operation is within 15 min so that the tubes prior to bending can be considered as W-temper (without natural aging). Similarly, for the experimental records, in R1 and R3, the transfer time between bending and post-bend-AA is also controlled within 15 min, although believed less important. To ensure more accuracy and

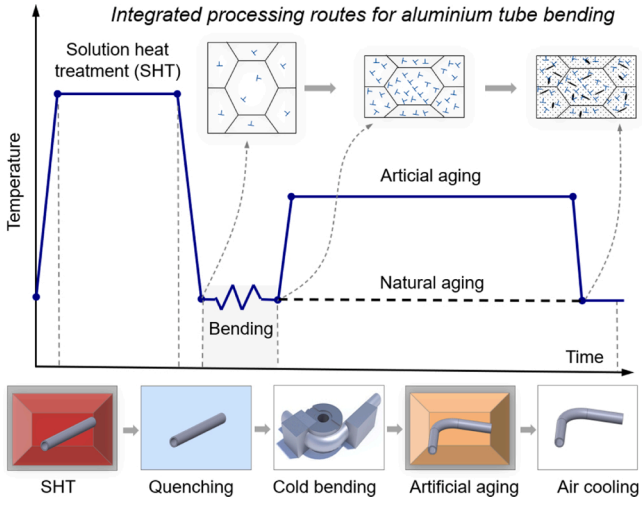


**Fig. 1.** Schematic illustration of integrated tube bending process.

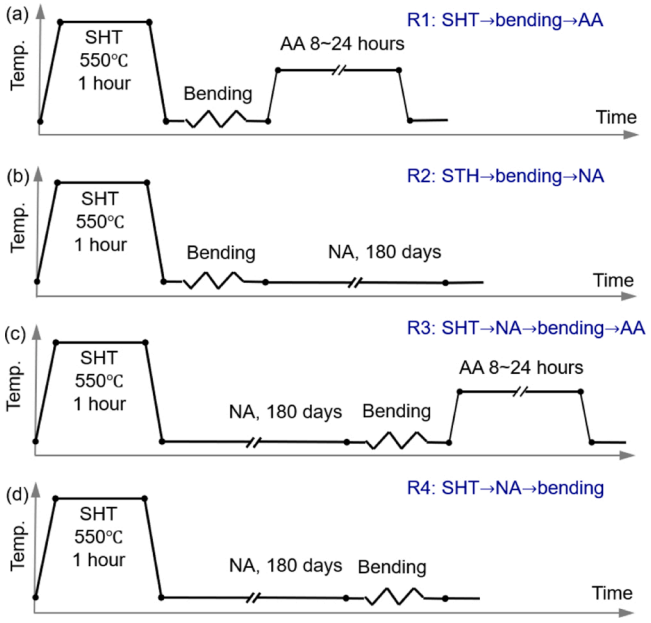


**Fig. 2.** Schematic of the different processing routes: (a) R1: SHT → bending → AA; (2) R2: SH → bending → NA; (c) R3: SHT → NA → bending → AA; (d) R4: SHT → NA → bending.

reliability of the experimental results, three workpieces have been tested for each experimental condition. For all the four processing routes above, the experimental details for thermal treatments and cold bending are described as follows:

#### 2.1.1. Thermal treatment experiments

The SHT experiments are conducted using a Nabertherm N41/H chamber furnace. The AA6060-T4 tubes are cut into segments with a length of 400 mm, and then placed into the furnace, and held at the solutionizing temperature of 550 °C for one hour. After SHT, the samples are quenched into a cold-water tank and kept for 10 min in order to obtain the supersaturated solid solution microstructure. The artificial aging experiments are performed in the Nabertherm N41/H chamber furnace. Based on the aging time-strength curves of AA6060 alloy reported in [28], the aging temperature is set at 170 ℃ and the holding periods are set as 8 (most common in the industry), 16, and 24 h. For natural aging, the tubes are stored at room temperature (indoor in an experimental laboratory) for 180 days.

#### 2.1.2. Rotary draw bending (RDB) experiments

RDB is one of the most widely used methods for forming bent tubular parts in different fields and applications. The principle of RDB is illustrated in Fig. 3(a). The tube is subjected to multi-tool constraints including bend die, clamp die, pressure die, wiper die, etc. Under the geometrical constraints of the tools, the tube is drawn around the bending center to form a bent tubular part with a certain bending radius and bend angle. After bending, the tube is unloaded by releasing the tools and springback occurs accordingly. A STAR EVO BEND 800 CNC bending machine, as shown in Fig. 3(b), employing bending dies with a radius of $R = 40$ mm ($R/D = 2.5$), is used. Considering that the diameter-to-thickness ratio ($D/t = 9.41$) is less than 20, the wrinkling and over-ovalization defects normally is less likely to occur to any

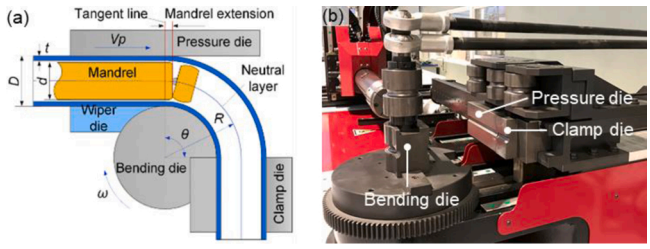


**Fig. 3.** RDB process: (a) bending principle; (b) machine and tooling system.

significant extent during bending. Thus, a mandrel and wiper dies are not used in the bending process. The bend angles are set as $\theta = [30, 60, 90, 120, 150]$ degree. The bending velocity is set as 25 degree per second, and the push velocity of the pressure die is kept proportional to the tangent velocity of the centerline of the tube.

### 2.2. Geometric dimensional measurements

For the bent tubes undergoing different thermal processing routes, the three main dimensional indices—i.e., springback, wall-thinning, and ovalization—are used to evaluate the geometrical characteristics. Fig. 4 (a) shows schematically the angular changes observed due to the springback upon unloading. For the angular dimensional measurement of the bent tubes, as shown in Fig. 4(b), a Leitz-PMM-C-600 coordinate measurement machine is used. It should be noted that both the springback angle after bending and the springback variation between samples undergoing the same thermal processing route are evaluated.

Fig. 4(c) and (d) show the cross-section cut from the center bend section ($\theta/2$ position) of the tube. During the RDB process, the outside wall of the bent tube is under tension and thus undergoes thinning, whereas the inside wall is under compression and undergoes thickening. Here the changes of thickness and outer diameter of the bent tubes are measured by using a slide caliper. At the same time, the cross-section of the tube is ovalized or flattened. In this study, the quality characteristics including springback, wall thickness, and cross-sectional ovalization are considered to represent the dimensional accuracy.

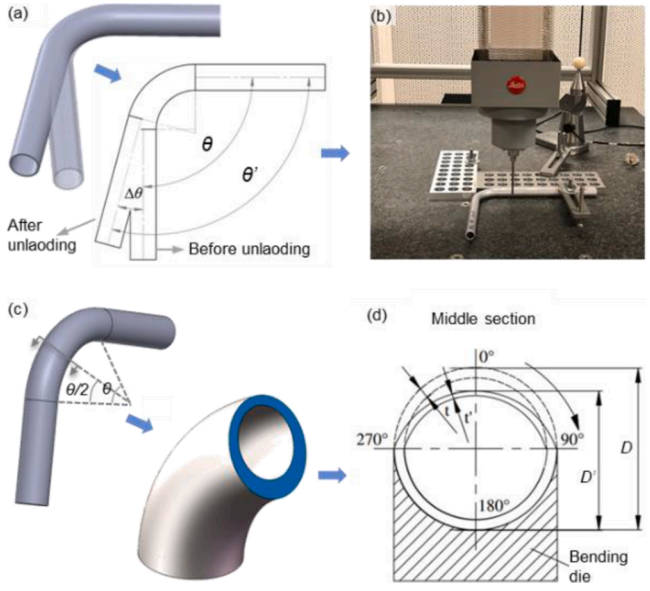


**Fig. 4.** Measurement of geometrical dimension: (a) springback angle; (b) CMM for springback measurement; (c) cross-section of bent tube; (d) wall thinning-thickening and ovalization.

### 2.3. Hardness measurements

The mechanical properties of the bent tubes are examined at the end of each processing route, using micro Vickers hardness (indentation) tests. Fig. 5(a) shows a ring sample for indentation tests, which is cut from the middle section of the bent tube. Fig. 5(b) illustrates the testing locations defined to examine the overall hardness distribution of bent tubular parts, including five representative locations at 0, 45, 90, 135, and 180 degree along the hoop direction of the ring sample. The ring samples are ground by SiC papers up to 4,000 grit, followed by diamond paste polishing with 3 μm and 1 μm particle size, and finalized by silica colloid suspension polishing (OPS, Struers) for about 20 min for each sample. After preparation, the indentation test is performed at the different locations using a Mitutoyo MicroWiZhard Vickers tester with 4 s loading time, 10 s holding time and 4 s unloading time at a maximum load of 1 kg. In each representative zone, a minimum of 6 indents in each region of interest is made to get some statistical reliability.

### 2.4. NaMo simulation

NaMo is a nanoscale material model for Al-Mg-Si series alloys with three interacting sub-models, i.e., a precipitation model, a yield strength model, and a work-hardening model, which enables accurate simulation of mechanical properties of the alloys that have undergone different thermal-mechanical histories [29–31]. The input to NaMo is the chemical composition and the given thermo-mechanical loading history of the alloy after the extrusion process, and the output is the stress-strain curves. NaMo models have been carefully verified by extensive experimental data [29–31]. In this study, the NaMo-Version 3 is employed to simulate the stress-strain curves of AAA6060 under different processing routes. The average chemical composition given in Table 1 is used as input of the alloy. Four representative thermo-mechanical loading histories are determined in the following based on the integrated processing routes described in Section 2.1.

- Case #1: AA6060-T4 → SHT, 550 ℃, 1 h → water quenching → NA, 0 h
- Case #2: AA6060-T4 → SHT, 550 ℃, 1 h → water quenching → NA, 180 d
- Case #3: AA6060-T4 → SHT, 550 ℃, 1 h → water quenching → NA, 0 h → deformation, $\varepsilon = 10$ % → NA, 180 d
- Case #4: AA6060-T4 → SHT, 550 ℃, 1 h → water quenching → NA, 0 h → deformation, $\varepsilon = 10$ % → AA, 170 ℃, 24 h

In these thermo-mechanical routes, the case strain induced by cold deformation is defined as 10 %, which is also about half of the maximum major strain during tube bending under the tooling setup given in Section 2.1. Fig. 6(b) shows the stress-strain curves of the AA6060 alloy obtained by NaMo simulation. The final states of Case #1 and Case #2 can be considered as W-temper and T4-temper, respectively. The yield

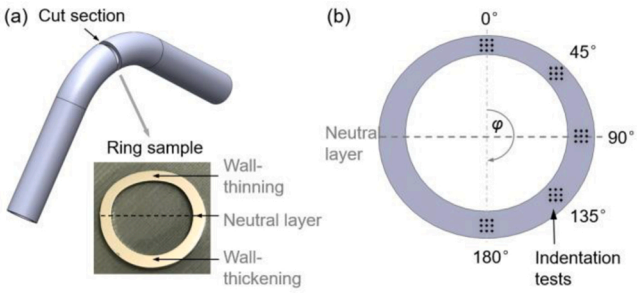


**Fig. 5.** Schematics illustrating characterization of mechanical properties: (a) sample preparation; (b) testing zones for indentation in the middle section of the bent tube.

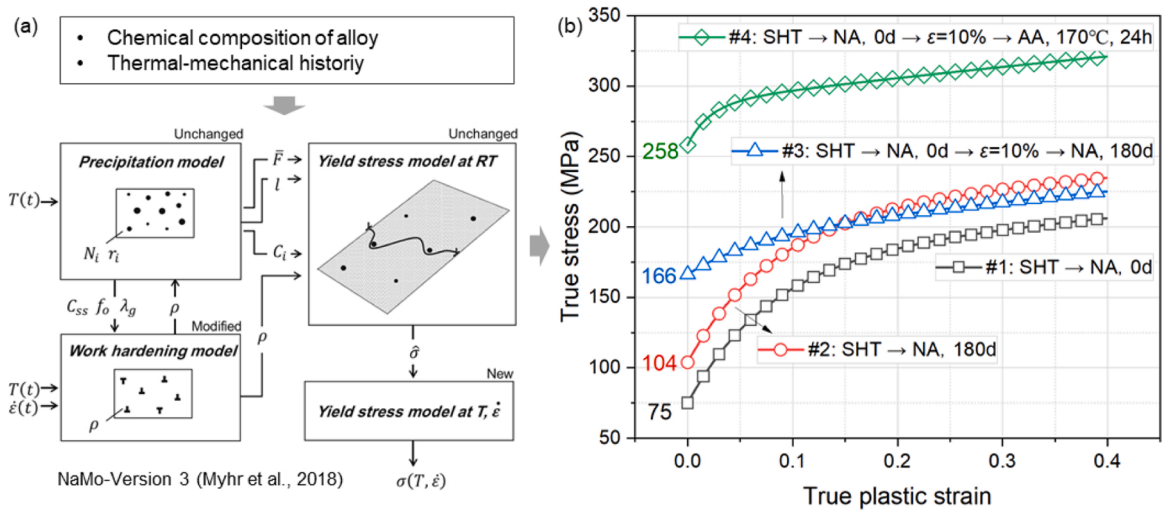


**Fig. 6.** NaMo simulation for AA6060 alloy: (a) schematic outline of NaMo model vers [30]; (b) stress-strain curves under different thermo-mechanical histories.

strengths in Case #1 and Case #2 are 75 MPa and 104 MPa respectively, meaning that the SHT treatment can reduce the yield strength of AA6060 alloy by about 28 % as compared to T4 material. In Case #3, the material is cold-deformed and then naturally aged to T4. Comparing the curves in Case #2 and Case #3, it can be found that the pre-deformation could significantly increase the yield strength but decrease the work-hardening effect. In Case #4, the W-temper material is deformed first and followed by the AA treatment. The curve for Case #4 shows that the post AA can dramatically increase the yield strength by about 150 % as compared to T4 material. As NaMo has been carefully calibrated by extensive previous experiments for Al-Mg-Si alloys, including AA6060, the overall characteristics of the curves predicted by NaMo are assumed to be accurate. These simulated stress-strain curves will provide a reference to help analyze the impact of the thermo-mechanical routes on quality characteristics well as to understand their underlying mechanisms.

## 3. Results and discussion

### 3.1. Evaluation of springback

Fig. 7 shows the bent tubular parts fabricated by different processing routes, i.e., (a) R1, (b) R2, and (c) R3 and R4. It is noted that none of the formed parts showed any occurrence of defects such as wrinkling or cracks. As the diameter-to-thickness ratio ($D/t = 9.4$) is relatively low and the bending radius ($R/D = 2.5$) is relatively high, thus, the formation of such defects is less likely to occur. To study the influence of different forming processes on springback, the bend angles of formed parts are evaluated in the following.

According to the schematics of angular angles during unloading, shown in Fig. 4(a), the springback angle ($\Delta\theta$) is defined as follows:

$$\Delta\theta = \theta' - \theta \tag{1}$$

where $\theta'$ denotes the final angle measured after springback, and $\theta$ denotes the bend angle preset in the bending machine.

As described in the above section, the SHT tubes without aging treatment (in short described as W-temper) are used in the bending

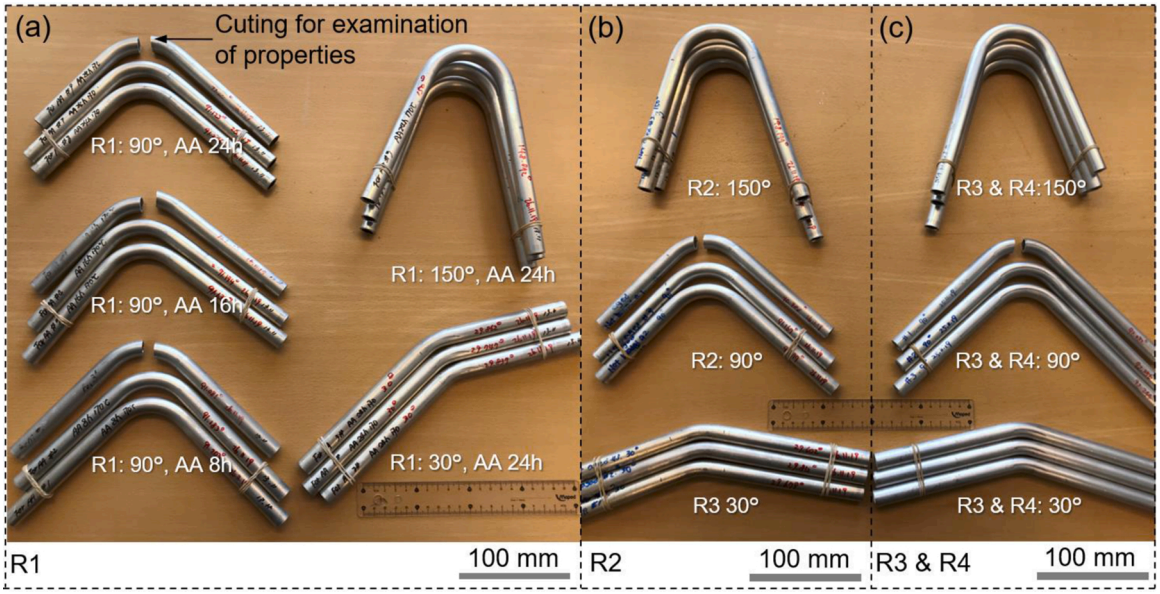


**Fig. 7.** Experimentally bent tubular parts: (a) R1; (b) R2; (c) R3 and R4.

operation in R1 and R3, while the samples naturally aged to T4-temper are used in the bending operation in R2 and R4. Thus, the springback angles of the tubes bent in W-temper in R1 and samples bent in T4-temper in R4 are compared in Fig. 8. For both temper conditions, the springback angle increases significantly with increasing the bend angle. When the bend angle increases from 30 to 150 degree, the increased springback of T4-temper tubes and W-temper tubes is 2.22 degree and 1.55 degree, respectively. The fact that the increase of springback of W-temper tubes is significantly less than that of the T4-temper ones indicates that the springback with bend angle is to some extent proportional to the nominal springback for a given bend angle. Comparing the springback for the same bend angle, it can be found that the T4-temper samples give a much higher springback angle than the W-temper ones. For bending at 30 degree, the springback of T4-temper tubes is about 75 % higher than that of W-temper tubes. Even though the relative difference trends to be lower with increased bend angle, the springback of the T4-temper tube is still about 45 % higher than that of the W-temper tubes for bending at an angle of 150 degree. Overall, the W-temper tubes can reduce springback by more than 50 % as compared to the T4-temper tubes. Here it should be noted that the latter represents the most common production strategy in today's manufacturing industry.

Such a large difference in springback is caused by the lower yield stress characteristic for solution-heat-treated AA6060 tubes. The yield strength-to-Young's modulus ratio is normally used as an index to roughly indicate the relative springback magnitude. Young's modulus is obviously insensitive to temper condition. However, as shown in Fig. 6 (b), the material strength undergoing natural aging is significantly changed, resulting in a higher strength-to-Young's modulus ratio and thus higher nominal springback and, thus, variations in springback.

The variation of springback during AA and NA treatments are compared. Fig. 9(a) shows the variation of springback angle measured after different AA cycles for tubes bent in W-temper in R1. It is observed that the change of springback during AA is within the error bands, confirming that the influence of AA on geometric dimensions of bent shapes is very low and the variations of the bent tubes during AA are less than 0.07 degree. Such a minor difference can be neglected for all practical purposes. Fig. 9(b) shows the angular variation of the bent tubes during NA in R2. It can be observed that, for the three bend angles of 30, 90, and 150 degree, the changes of bend angles present an overall decreasing trend as storage time increases. The maximum angular variation measured after NA is about 0.2 degree. Even though the variation during NA is a little higher than that during AA, it still can be considered negligible in most cases, particularly when seen in comparison with the impact of other variations such as material properties.

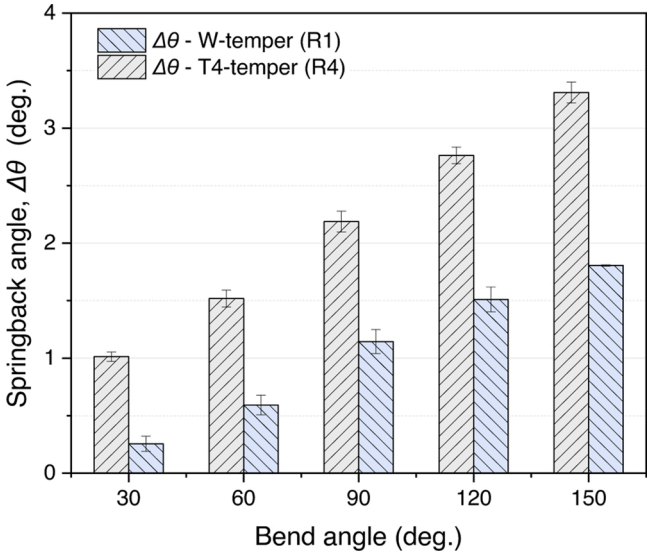


**Fig. 8.** Springback comparison of T4-temper and W-temper tubes.

The change of angles or curvatures of bent shapes with storage time is also called 'time-dependent springback'. Despite several past studies on time-dependencies of springback, the underlying mechanisms are still not understood sufficiently [32]. It is proposed that creep relaxation behavior driven by residual stress of the formed parts plays an important role in this phenomenon [33]. As the strength of W-temper tubes is relatively low, the residual stress of tubes bent in W-temper is also low. When the bent tubes undergo aging, the accumulated precipitations with aging time can significantly increase the strength of bent tubes, making the preserved low residual stress cannot provide enough 'driving force' for creating dimensional changes in the bent shapes. Thus, a low level of angular variation of the tubes bent in W-temper during AA and NA processes is observed in this study.

### 3.2. Evaluation of thickness change and cross-sectional ovalization

Wall-thinning and ovalization of bent tubular products are to be defined before further evaluation of results. According to the schematic shown in Fig. 4(d), normalized wall-thinning ($\eta_t$) and ovalization ($\eta_D$) in the middle section are given in the following equations, respectively:

$$\eta_t = \Delta t/t = (t' - t)/t \tag{3}$$

$$\eta_D = \Delta D/D = (D - D')/D \tag{4}$$

where $\Delta t$ is the change of thickness during the bending process, and $t$ and $t'$ are wall thickness before and after bending, respectively; $\Delta D$ is the change of outer diameter (taken perpendicular to the bending axis), and $D$ and $D'$ are outer diameter measured before and after bending, respectively.

The bent tubes with a nominal preset bend angle of 90 degree are used to analyze the wall-thinning of extrados and cross-sectional ovalization. As shown in Fig. 10(a) and (b), the normalized wall-thinning and normalized cross-section ovalization are at a similar level for the parts bent in W-temper in R1 and R2. As compared with tubes bent in T4-temper in R3 and R4, it can be found that the ovalization of bent tubes obtained by R1 and R2 is about 22 % higher. However, the wall-thinning in R1 and R2 is about 26 % lower than that in R3 and R4. Welo and Paulsen [34] revealed that the main parameters controlling the maximum ovalization in tube bending include the following: tube diameter, thickness, bending radius, and work-hardening exponent of tubular material. Here increasing work-hardening exponent was found to cause more severe ovalization. As shown in Fig. 6(b) for the AA6060 alloy, the work-hardening exponent of the W-temper (R1 and R2) is 0.28, which is higher than the T4-temper (R3 and R4) with an exponent of 0.24. Thus, the ovalization of bent parts in R1 and R2 is more pronounced than that of R3 and R4. At the same time, as more pronounced ovalization occurs, the bending curvatures of fibers in the outside zone of the cross-section are reduced, which again reduces the longitudinal strain causing less wall-thinning for W-temper tubes. Overall, as compared with the commonly used R4 process, the R1 (and R2) processes with bending of W-temper tubes show increased ovalization but can give less wall-thinning of the bent tube at the same time.

### 3.3. Evaluation of product strength

The final formed bent tubular parts have undergone both cold deformation and aging including NA, or AA, or both. Consequently, the final strength of the products is determined by the combined deformation-induced work-hardening effect and the aging-induced precipitation-hardening effect. Before discussing the product strength under different processing routes, the contributions made by deformation and precipitation to the final strength of AA6060 alloy is briefly illustrated in Eq. (5), as given in the following:

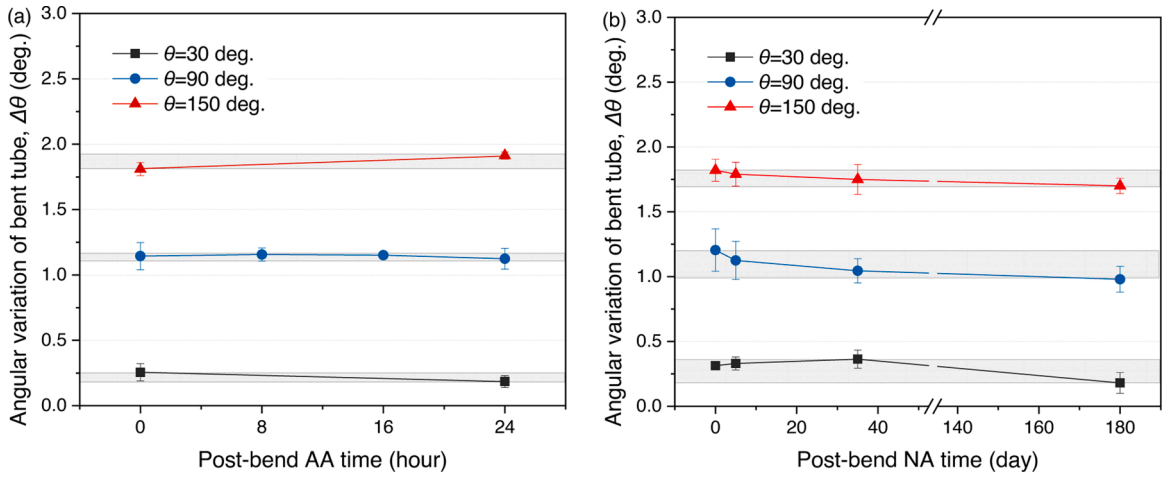


**Fig. 9.** Angular variation during post aging: (a) artificial aging; (b) natural aging.

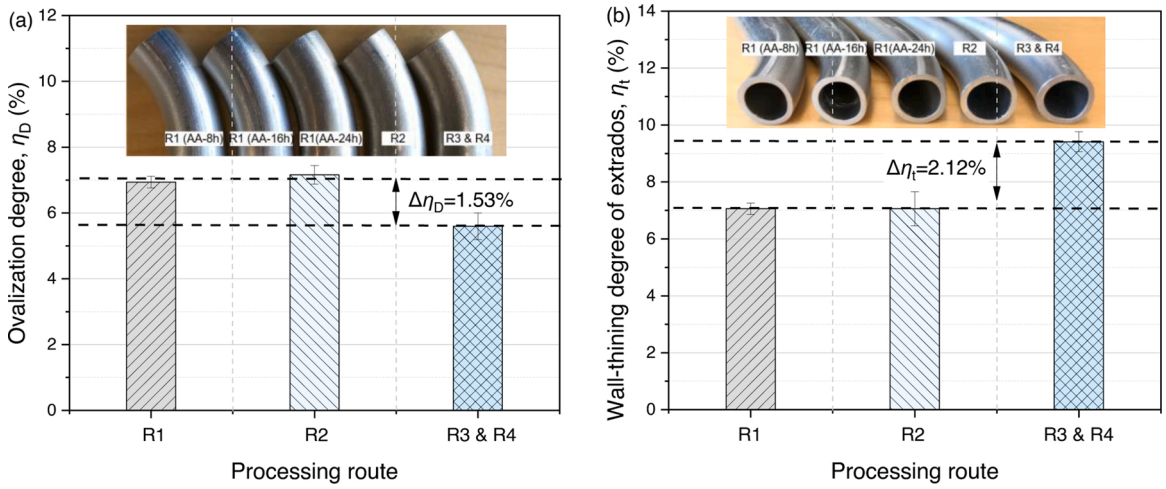


**Fig. 10.** Ovalization and wall-thinning of bent tubes: (a) ovalization of cross-section; (b) wall-thinning of extrados.

$$\sigma = \sigma_0 + \Delta\sigma_{ss} + \Delta\sigma_d + \Delta\sigma_p \quad (5)$$

where $\sigma$is the final yield strength (0.2 % offset proof stress), $\sigma_0$ is the so-called friction stress in aluminium and is normally considered as a constant value, $\Delta\sigma_{ss}$ is the solid solution strength addition, $\Delta\sigma_d$ is the deformation strength addition, and $\Delta\sigma_p$ is the precipitation strength addition.

By re-organizing the stress-strain curves illustrated in Fig. 6, the different contributions to the final yield strength for AA6060 alloy under different thermo-mechanical histories can be obtained, as shown in Fig. 11. In this study, for any thermo-mechanical history applied, the reference base point is SHT. Thus, the solid solution strength addition $\Delta\sigma_{ss}$ is constant. For the deformation strength addition $\Delta\sigma_d$ and precipitation strength addition$\Delta\sigma_p$, these contributions depend on the loading sequence and aging treatment methods applied. As illustrated in Fig. 11, taking the R1 route as an example, the schematic view of the material hardening path is from O to A, and further to D. In the following, the theory briefly reviewed herein will be used as a reference in analyzing the impact of processing routes on the product strength.

Here hardness distribution is used to evaluate the strength of the formed tubular parts. As described in Section 2.3, the longitudinal hardness distributions along the hoop direction of the cross-section of the bent tubes are examined. The hardness distributions of the bent parts formed by different processing routes are illustrated in Fig. 12.

Firstly, the average hardness of the five representative zones ($\varphi$ = 0, 45, 90, 135, 180) is analyzed to evaluate the overall strength of the formed parts. It is well known that AA can significantly accelerate the formation of precipitation, and the mechanical properties obtained by AA treatment is much higher than that obtained by NA treatment. Thus, the overall strength of the artificially-aged bent parts is significantly higher than that of the naturally-aged ones, as shown in Fig. 12. Given this fact, the four processing routes are classified into two groups in the following context to analyze the product hardness; i.e., naturally-aged tubes including R2 and R4 (final formed tubes in T4 condition), and artificially-aged ones including R1 and R3 (final formed tubes in T6 condition).

For the artificially-aged group (R1 and R3), the average hardness of the bent shapes formed by R1 is 74 (HV), which is about 10 % lower than that obtained by route R3. According to the material strength contribution shown in Fig. 11, the strength difference of the bent tubes in R1 and R3 is that the latter has undergone a pre-NA treatment prior to the bending operation. The effect of pre-NA treatment on in achieving a higher strength of the Al-Mg-Si series alloys with lower Mg and Si content, for instance, AA6060 alloy and AA6063 alloy, is also confirmed by Martinsen et al. [35]. The reason behind this phenomenon lies in the fact that the kinetics of precipitation during AA depends on the quantity and the type of Mg/Si clusters [36]. In R3 route, some Mg/Si clusters created during the previous NA process can serve as nuclei for the precipitation of particles during subsequent AA process. As a result, the total precipitation strength addition in R3 is higher than that in R1. It

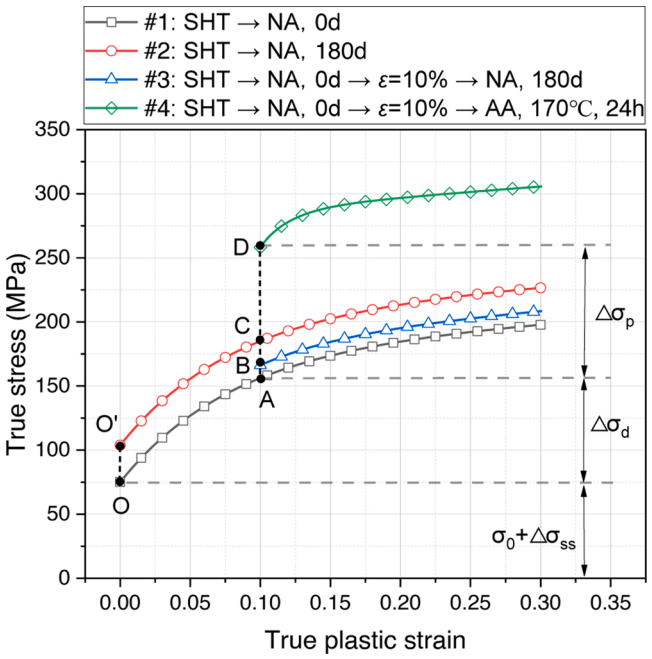


**Fig. 11.** Analysis of strength additions in AA6060 under different thermo-mechanical histories.

should be noted that a well-known transient negative NA effect normally occurs under the 'NA + AA' treatment when the Al-Mg-Si alloys are undergoing NA for less than about 10 h. Martinsen et al. [35] comparatively studied the transient negative NA effect in Al-Mg-Si alloys with high, medium, and low solute content, and revealed that both transition period and the strength decrease induced by the negative NA effect are more pronounced for the alloys with a higher solute content. For the low-solute content AA6060 alloy, the strength decrease is quite minor and the transition length is very short, which provides the possibility to make the overall mechanical properties of parts formed by R3 higher than that those formed by R1. However, as the pre-deformation is introduced before AA, resulting in a complex triple-effect of pre-deformation, NA, and AA on material strength, which is not considered in that study. Therefore, when it comes to the design of thermal processing route for customized high-strength products, the complex effect of NA, AA, and deformation on strength of the given alloys should be identified, and the parameters used for NA and AA need to carefully chosen to reduce the strength loss caused by the negative effect of NA.

For the naturally-aged group (R2 and R4), the average hardness of the tubes formed by R2 is about 53 (HV), which is about 20 % lower than that of the parts formed by R4. As introduced in Section 2, R2 represents the SHT tubes are bent first and followed by NA, while R4 the NA is prior to bending operation, that is, pre-deformation before NA can reduce the material strength with relative to pre-NA before deformation. As shown in Fig. 11, the hardening path of R2 follows O→A→B and the hardening path of R4 follows O→O'→B. It is known that the strength of Al-Mg-Si alloys can be significantly increased during NA due to the formation of a high number density of GP zones. When the AA6060 alloys have undergone both plastic deformation and NA, both increased dislocation density and precipitation can contribute to improved strength. Kolar et al. [37] studied the coupled effect of pre-deformation and NA on AA6060 alloy and revealed that the increase in yield stress due to NA is decreased when the pre-deformation is increased from 0 to 10 %, which also agrees with the results of the present work. When the deformation occurs before NA, the main contribution to the increased strength is made by the increased dislocation density due to pre-deformation and to lower extent by the formation of GP zones. Such a phenomenon is attributed to, that is, the precipitates formed in the pre-deformed material may be fewer and coarser due to accelerated preferential nucleation on dislocations, thus making the hardness obtained by R4 is higher than that obtained by R2.

Moreover, the hardness distribution along the hoop direction in the cross-section of bent tubes is analyzed. It can be found from Fig. 12 that there seems to be no substantial difference between the five representative zones ($\varphi = 0$, 45, 90, 135, 180) for the bent tubes formed by R1 and R3 processes, showing a uniform distribution along the hoop direction of the cross-section. This indicates the limited influence of bending-induced deformation on mechanical properties after artificial aging. However, for the naturally-aged group (R2 and R4), the hardness distribution of bent shapes presents a clear trend; the hardness is lower around $\varphi = 90$ degree (near neutral layer upon bending), and higher at $\varphi = 0$ degree (extrados) and $\varphi = 180$ degree (intrados), which is different from the results obtained for the artificially-aged specimens. The difference in hardness distribution around the perimeter of the cross-section for the artificially-aged and the naturally-aged groups is attributed to the significantly improved contribution made by AA to material strengthening. For the AA6060 alloy undergoing coupled NA and deformation, the work-hardening still dominates the strengthening of material so that a non-uniform hardness distribution is obtained in R2 and R4. For the material that underwent coupled pre-deformation and AA, however, the contribution of precipitation hardening becomes much more significant due to the formation of a high number density of post-

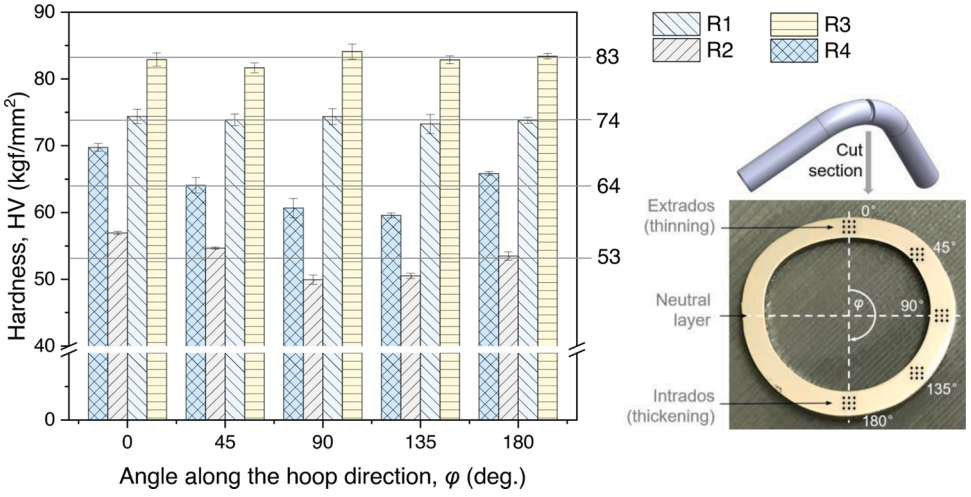


**Fig. 12.** Hardness (HV) of bent tubes formed by different processing routes.

$\beta''$ precipitates in the pre-deformed condition as reported by Teichmann et al. [38], resulting in a uniform distribution of hardness in the cross-section of tubes formed by R1 and R3.

### 3.4. Application prospects and proposals of the integrated tube bending process

Based on the analysis in Section 3.1~3.3, the processing route R1 both minimizes the springback and provides higher mechanical strength, as well as creates a more uniform strength distribution. However, R1 also comes with a drawback; that is, the cross-sectional ovalization level is higher than that for the commonly used forming strategies utilizing as-received T4-temper materials in bending. However, the ovalization problem could be addressed or suppressed by an optimized design of tooling and process parameters. Normally, for the manufacturing of bent tubular parts with strict dimensional requirements for ovalization, mandrel tools can be used in many bending processes to control this ovalization problem [11,17,39,40]. For the bending of micro-tubes, a micro-wire type of mandrel could also be applied [41]. In addition to the tooling design, the additional axial push-assistant force can be applied in the rotary draw bending process to help suppress ovalization [39]. Overall, from the perspective of product design by addressing 'dimensional accuracy-driven' and 'product property-driven' requirements, the R1-type integrated forming processes (bending in W-temper and followed by AA) can provide more potential to achieve this goal.

Another advantage of R1-type integrated forming processes is that the alloys in W-temper normally can significantly improve the cold ductility [42], which increases the bendability and thus improves the possibility to manufacture tight-radius bends. Such tight-radius bent parts, however, is very difficult to fabricate in T4 or T6 conditions. Furthermore, from the view of lean production, R1-type processes with using post AA treatment can shorten the entire production cycle, reducing the 'waiting time'—one of the seven wastes in lean manufacturing [43].

The integrated forming process proposed herein can be used for manufacturing bent tubular parts with different tube geometry, including thick-walled, thin-walled, and various section tubes, etc. Even though only a specific tube geometry is tested in this study, the knowledge gained is applicable for the design and development of the bending process for a wide range of tube geometries. When the integrated forming process is used to bend a tube with a specific geometry, some necessary modifications are needed with regard to the tooling design in bending operation and parameter optimization in thermal treatments. For example, mandrel and wiper tools are normally used in bending of thin-walled or ultra-thin-walled tubes to avoid the wrinkling defect and over-ovalization. For the thermal treatments, the thermal-related parameters need to be identified to assure the mechanical properties of the formed products as well as to meet requirements for production efficiency, process capability, and cost, etc. In this regard, the alloy compositions, the size of parts, etc., should be taken into account.

It should be noted that the practical issues concerning the design and development of products and processes are more complex than described above. In industrial practice, however, more factors need to be carefully considered and comprehensively assessed in the selection of alternative production processes, as well as in the design of the optimal processing routes for a formed component. Examples of such contextual, practical factors are (degree of) vertical integration, supply chain and logistics, supplier base, inhouse manufacturing (bending) capability, in-house heat-treatment capability, product costs, product volume, equipment investments (e.g. ovens for heat treatment), etc.

## 4. Conclusions and outlook

Achieving the desired dimensional accuracy and mechanical properties is one of the most significant aspects in metal forming. In this research, we aim to provide new insights into the impact of thermo-mechanical processing routes on product quality in the integrated bending process for aluminium tubes. For this purpose, a series of carefully-controlled experiments with different processing routes, integrating solution-heat-treatment (SHT), artificial aging (AA), natural aging (NA), and cold bending, are designed. The main conclusions are summarized as follows:

- As compared with the conventional production strategy of employing T4-temper tubes in the bending operation, solutionzing immediately *before* bending can minimize the springback by more than 50 % and reduce the wall-thinning by about 26 %. However, this comes at the expense of increased cross-sectional ovalization by about 22 % for SHT.
- The tubes naturally aged *before* bending and artificially aged *after* bending can improve the hardness by 16 % averaged over the samples bent in W-temper and subsequently artificially aged. For product strength without AA, the hardness of samples naturally aged to T4 *before* bending is 20 % higher than the samples stored and naturally aged to T4 *after* bending.
- When using AA, this creates a uniform distribution of hardness in the cross-section of bent tubes, almost independent of the non-homogeneous pre-deformation imposed by bending. When supplying parts in T4-temper using AA, there is a non-homogenous distribution of hardness, however, highly dependent on local pre-deformation of the material.
- From the perspective of product design in terms of both geometrical and mechanical requirements—the overall motivation for this study—SHT immediately *before* bending in combination with subsequent AA *after* bending provides more flexibility and potential for improving shape accuracy, setting customized properties, and making tight-radius parts. This flexibility comes at a higher investment and operational cost, though, due to the SHT step in the process.

The integrated processing strategy proposed herein can be used for manufacturing bent tubular parts with different tube geometry including thick-walled, thin-walled, and various section ones. It is believed that the knowledge created in this study makes a contribution to the selection and design of more suitable, efficient processing routes for aluminium tube bending beyond the cases tested herein.

However, the present work is mainly limited in scope to the impact of processing routes on product quality. The robust design of products and processes call for a more comprehensive study on the particular influential parameters related to these routes. One important topic in this connection is optimizing the AA temperature for reducing the production time for providing consistent product quality in terms of dimensional accuracy and mechanical properties.

## CRediT authorship contribution statement

**Jun Ma:** Conceptualization, Methodology, Investigation, Formal analysis, Writing - original draft, review and editing. **Torgeir Welo:** Conceptualization, Methodology, Investigation, Supervision, Writing - review and editing. **Di Wan:** Investigation – experiment, Writing - review and editing.

## Declaration of Competing Interest

The authors declare that they have no known competing financial interests or personal relationships that could have appeared to influence the work reported in this paper.

## Acknowledgements

The authors gratefully acknowledge the financial support from

Norwegian University of Science and Technology (NTNU), NTNU Aluminium Product Innovation Center (NAPIC) and the KPN Project VALUE (No. 267768) sponsored by Research Council of Norway, Hydro and Alcoa. In addition, the authors would like to thank Prof. Ole Runar Myhr at Hydro and Mr. Anders Nesse at SINTEF Manufacturing for the help in NaMo simulation, and Dr. J. Blindheim and Mr. T. Ha at NTNU for the help in conducting the experiments.

## References

[1] Cao J, Banu M. Opportunities and challenges in metal forming for lightweighting : review and future work. J Manuf Sci Eng 2020;142:1–24. https://doi.org/10.1115/1.4047732.
[2] Welo T, Ringen G, Ma J. An overview and evaluation of alternative forming processes for complex aluminium products. Procedia Manuf 2020;48:82–9. https://doi.org/10.1016/j.promfg.2020.05.022.
[3] Zheng K, Politis DJ, Wang L, Lin J. A review on forming techniques for manufacturing lightweight complex d shaped aluminium panel components. Int J Light Mater Manuf 2018;1:55–80. https://doi.org/10.1016/j.ijlmm.2018.03.006.
[4] Li H, Fu MW. Deformation-based processing of materials: behavior, performance, modeling, and control. Elsevier; 2019. https://doi.org/10.1016/C2017-0-01559-8.
[5] Li H, Yang H, Zhang ZY, Li GJ, Liu N, Welo T. Multiple instability-constrained tube bending limits. J Mater Process Technol 2014;214:445–55. https://doi.org/10.1016/j.jmatprotec.2013.09.027.
[6] Ma J, Welo T. Analytical springback assessment in flexible stretch bending of complex shapes. Int J Mach Tools Manuf 2020;160:103653. https://doi.org/10.1016/j.ijmachtools.2020.103653.
[7] Allwood JM, Duncan SR, Cao J, Groche P, Hirt G, Kinsey B, et al. Closed-loop control of product properties in metal forming. CIRP Ann Manuf Technol 2016;65:573–96. https://doi.org/10.1016/j.cirp.2016.06.002.
[8] Yang H, Li H, Zhang Z, Zhan M, Liu J, Li G. Advances and trends on tube bending forming technologies. Chinese J Aeronaut 2012;25:1–12. https://doi.org/10.1016/S1000-9361(11)60356-7.
[9] Liu H, Liu Y. Cross section deformation of heterogeneous rectangular welded tube in rotary draw bending considering different yield criteria. J Manuf Process 2021;61:303–10. https://doi.org/10.1016/j.jmapro.2020.11.015.
[10] Zeng Y, Li Z. Experimental research on the tube push-bending process. J Mater Process Technol 2002;122:237–40. https://doi.org/10.1016/S0924-0136(02)00027-4.
[11] Ghiotti A, Simonetto E, Bruschi S, Bariani PF. Springback measurement in three roll push bending process of hollow structural sections. CIRP Ann Manuf Technol 2017:3–6. https://doi.org/10.1016/j.cirp.2017.04.119.
[12] Miller JE, Kyriakides S, Bastard AH. On bend-stretch forming of aluminum extruded tubes - I: experiments. Int J Mech Sci 2001;43:1283–317. https://doi.org/10.1016/S0020-7403(00)00039-4.
[13] Guo X, Xiong H, Li H, Xu Y, Ma Z, El-aty AA, et al. Forming characteristics of tube free-bending with small bending radii based on a new spherical connection. Int J Mach Tools Manuf 2018;133:72–84. https://doi.org/10.1016/j.ijmachtools.2018.05.005.
[14] Hashemi R, Niknam SA. Flexible bending of rectangular profiles: numerical and experimental investigations. J Manuf Process 2020;56:390–9. https://doi.org/10.1016/j.jmapro.2020.04.072.
[15] Ghiotti A, Simonetto E, Bruschi S. Insights on tube rotary draw bending with superimposed localized thermal field. CIRP J Manuf Sci Technol 2021;33:30–41. https://doi.org/10.1016/j.cirpj.2021.02.012.
[16] Tao Z, Li H, Ma J, Yang H, Lei C, Li G. FE modeling of a complete warm-bending process for optimal design of heating stages for the forming of large-diameter thin-walled Ti-6Al-4V tubes. Manuf Rev 2017:4. https://doi.org/10.1051/mfreview/2017010.
[17] Xu X, Wu K, Wu Y, Fu C, Fan Y. Push-bending method development of thin-walled tube with relative bending radius of 1 using sectional elastomers as mandrel. Int J Adv Manuf Technol 2019:995–1008. https://doi.org/10.1007/s00170-019-04266-0.
[18] Li H, Yang H, Ma J, Li G, Huang D. Breaking bending limit of difficult-to-form titanium tubes by differential heating-based reconstruction of neutral layer shifting. Int J Mach Tools Manuf 2021.
[19] Zhou W, Yu J, Lin J, Dean TA. Manufacturing a curved profile with fine grains and high strength by differential velocity sideways extrusion. Int J Mach Tools Manuf 2019;140:77–88. https://doi.org/10.1016/j.ijmachtools.2019.03.002.
[20] Lin C, Chu G, Sun L, Chen G, Liu P, Sun W. Radial hydro-forging bending: a novel method to reduce the springback of AHSS tubular component. Int J Mach Tools Manuf 2020:103650. https://doi.org/10.1016/j.ijmachtools.2020.103650.
[21] Lin J., Dean, Trevor A, Garrett, Richard P, Foster, Alistair D. Process For Forming Metal Alloy Sheet Components, British Patent, WO2008/059242A2, 2008.
[22] Li N, Zheng J, Zhang C, Zheng K, Lin J, et al. Investigation on fast and energy-efficient heat treatments of AA6082 in HFQ processes for automotive applications. MATEC Web Conf 2015:0–6. 05015.
[23] Li H, Yang J, Chen G, Liu X, Zhang Z, Li G, et al. Towards intelligent design optimization : Progress and challenge of design optimization theories and technologies for plastic forming. Chinese J Aeronaut 2020. https://doi.org/10.1016/j.cja.2020.09.002.
[24] Li N., Zheng J., Zheng K., Lin J, Davies C. A fast ageing method for stamped heat-treatable alloys, US Patent, US20180223405A1, 2018.
[25] Bourget JP, Fafard M, Shakeri HR, Côté T. Optimization of heat treatment in cold-drawn 6063 aluminium tubes. J Mater Process Technol 2009;209:5035–41. https://doi.org/10.1016/j.jmatprotec.2009.01.027.
[26] Sert A, Gürgen S, Çelik ON, Kuşhan MC. Effect of heat treatment on the bending behavior of aluminum alloy tubes. J Mech Sci Technol 2017;31:5273–8. https://doi.org/10.1007/s12206-017-1020-5.
[27] Ma J, Ha T, Blindheim J, Welo T, Ringen G, Li H. Exploring the influence of pre/post-aging on springback in Al-Mg-Si alloy tube bending. Procedia Manuf 2020;47:774–80. https://doi.org/10.1016/j.promfg.2020.04.239.
[28] Hydro. Technical datasheet - extruded products alloy EN AW - 6060. AlMgSi; 2019. p. 3–5.
[29] Myhr OR, Grong Ø, Pedersen KO. A combined precipitation, yield strength, and work hardening model for Al-Mg-Si alloys. Metall Mater Trans A Phys Metall Mater Sci 2010;41:2276–89. https://doi.org/10.1007/s11661-010-0258-7.
[30] Myhr OR, Grong Ø, Schäfer C. An extended age-hardening model for Al-Mg-Si alloys incorporating the room-temperature storage and cold deformation process stages. Metall Mater Trans A Phys Metall Mater Sci 2015;46:6018–39. https://doi.org/10.1007/s11661-015-3175-y.
[31] Myhr OR, Hopperstad OS, Børvik T. A Combined Precipitation, Yield Stress, and Work Hardening Model for Al-Mg-Si Alloys Incorporating the Effects of Strain Rate and Temperature. Metall Mater Trans A Phys Metall Mater Sci 2018;49:3592–609. https://doi.org/10.1007/s11661-018-4675-3.
[32] Wang JF, Wagoner RH, Carden WD, Matlock DK, Barlat F. Creep and anelasticity in the springback of aluminum. Int J Plast 2004;20:2209–32. https://doi.org/10.1016/j.ijplas.2004.05.008.
[33] Hama T, Suzuki T, Nakatsuji Y, Sakai T, Takuda H. Time-dependent springback of various sheet metals: an experimental study. Mater Trans 2020;61:941–7. https://doi.org/10.2320/matertrans.MT-M2019283.
[34] Welo T, Paulsen F. Predicting tube ovalization in cold bending: an analytical approach. Key Eng Mater 2015;651–653:1146–52. https://doi.org/10.4028/www.scientific.net/KEM.651-653.1146.
[35] Martinsen FA, Ehlers FJH, Torsæter M, Holmestad R. Reversal of the negative natural aging effect in Al-Mg-Si alloys. Acta Mater 2012:60. https://doi.org/10.1016/j.actamat.2012.07.047.
[36] Fujda M, Matvija M, Glogovský M. Effect of natural aging on mechanical response of the artificially aged EN AW 6063 aluminium alloy. Mater Sci Forum 2019;952:74–81. https://doi.org/10.4028/www.scientific.net/MSF.952.74.
[37] Kolar M, Pedersen KO, Brüggemann T. The effect of deformation on the work hardening behaviour after aging of two commercial Al-Mg-Si alloys. Mater Sci Forum 2010;642:261–6. https://doi.org/10.4028/www.scientific.net/MSF.638-642.261.
[38] Teichmann K, Marioara CD, Andersen SJ. The effect of preaging deformation on the precipitation behavior of an Al-Mg-Si alloy. Metall Mater Trans A 2012;43:4006–14. https://doi.org/10.1007/s11661-012-1235-0.
[39] Li H, Ma J, Liu BY, Gu RJ, Li GJ. An insight into neutral layer shifting in tube bending. Int J Mach Tools Manuf 2018:126. https://doi.org/10.1016/j.ijmachtools.2017.11.013.
[40] Li H, Yang H, Zhan M, Sun Z, Gu R. Role of mandrel in NC precision bending process of thin-walled tube. Int J Mach Tools Manuf 2007;47:1164–75. https://doi.org/10.1016/j.ijmachtools.2006.09.001.
[41] Roein M, Elyasi M, Mirnia MJ. Development of bending of AISI 304L micro-tubes with micro-wire mandrel and investigation of its effective parameters. J Manuf Process 2021;64:723–38. https://doi.org/10.1016/j.jmapro.2021.02.029.
[42] Kolar M, Pedersen KO, Gulbrandsen-dahl S, Teichmann K, Marthinsen K. Effect of pre-deformation on mechanical response of an artificially aged Al-Mg-Si alloy. Mater Trans 2011;52:1356–62. https://doi.org/10.2320/matertrans.L-MZ201127.
[43] Welo T, Ringen G. Beyond waste elimination : assessing lean practices in product development. Procedia CIRP 2016;50:179–85. https://doi.org/10.1016/j.procir.2016.05.093.